

The effectiveness of  $\text{Fe}^{3+} \rightarrow \text{Ho}^{3+}$  energy transfer is more readily determined if the  $\text{Fe}^{3+}$  content is reduced. Comparison of the absorption and  $\text{Ho}^{3+}$  excitation spectra for YGaG containing 10% Fe and 2% Ho shows that the fluorescence quantum efficiency is near unity when exciting the  $\text{Fe}^{3+}$  absorption band centered at  $0.9 \mu$  (Fig. 16). The efficiency is also high for the band at  $0.7 \mu$ , but this band is obscured in absorption by an overlapping band due to an unknown defect. However, these efficiencies cannot be maintained in YIG due to excess  $\text{Fe}^{3+}$  absorption near the surface. Therefore, for

fluorescence studies at low temperature or cw maser experiments, radiation below  $1 \mu$  must be rejected.

### ACKNOWLEDGMENTS

We are pleased to acknowledge many helpful discussions with Dr. C. G. B. Garrett. We also express our appreciation to C. R. Radice, Jr., C. R. Staton, and R. A. Thomas for experimental assistance, Miss D. M. Dodd for zero-field absorption data, and E. M. Kelly for assistance with the growth of crystals.

## Spin Relaxation of $\text{Cr}^{3+}$ in $\text{MgO}$ : Evidence for Localized Modes\*

R. L. HARTMAN AND J. S. BENNETT

*Physical Sciences Laboratory, Redstone Arsenal, Alabama 35809*

AND

J. G. CASTLE, JR.

*University of Alabama in Huntsville, Alabama 35807*

(Received 31 October 1969)

Measurements of the relaxation of  $\text{Cr}^{3+}$  spins in cubic sites in  $\text{MgO}$  have been extended by fast pulsed saturation up to 180 K and by line broadening from 130 to 430 K. Explanations based on harmonic lattice vibrations must be modified to account for an observed linear dependence of  $1/T_1$  on  $T$  above 350 K. The relaxation is accurately given over seven decades of  $T_1$  by  $1/T_1 = AT + F(n) + B \text{csch}(\Delta/T)$ , where  $A = 0.93 \text{ sec}^{-1} \text{ K}^{-1}$ ,  $B = 1.20 \times 10^7 \text{ sec}^{-1}$ ,  $\Delta = 537 \pm 5 \text{ K}$ . The expected Raman relaxation function  $F(n)$  accounts for more than 50% of the relaxation only between 30 and 40 K, and could have the usual form  $T^n J_{n-1}$  with  $n = 5$  or  $7$ . Apparently, motions localized around each  $\text{Cr}^{3+}$  ion dominate the ground-state relaxation. The  $\text{csch}$  function suggests relaxation via localized modes having temperature-independent amplitudes. The localized mode frequencies coincide with a high-density region found in the vibronic sideband of the  $R$  line of  $\text{Cr}^{3+}$  in  $\text{MgO}$ .

### I. INTRODUCTION

THE possibility of introducing inaccuracies into calculations of spin relaxation time by use of harmonic phonon spectra was pointed out by Van Vleck<sup>1</sup> in a discussion on chrome alum: "Conceivably the oscillations most active in modulating the cluster  $\text{Cr} \cdot 6\text{H}_2\text{O}$  are not typical of the crystal as a whole and have a different distribution law." A theoretical description of localized vibrational modes in crystals was given soon after that by Lifshitz.<sup>2</sup> Effects of localized vibrations have been observed in a variety of ways, including spin relaxation,<sup>3,4</sup> optical spectra,<sup>5</sup> infrared absorption,<sup>6</sup> and

Raman scattering of laser light.<sup>7</sup> The pertinent vibrations have been discussed recently by Maradudin<sup>8</sup> in terms of three classes: localized modes, gap modes, and resonance modes. We find it necessary to consider effects of localized vibrations in order to explain the temperature dependence of the spin relaxation of  $\text{Cr}^{3+}$  in  $\text{MgO}$ .

The purpose of this paper is to report rather extensive observations of spin relaxation of  $\text{Cr}^{3+}$  in cubic sites in  $\text{MgO}$ . We offer an interpretation which accurately fits all the data and in retrospect seems simpler than the usual calculation of complete lattice sums.<sup>1,4</sup> The model attributes almost all of the observable relaxation above 40 K to a narrow frequency band of localized vibrations. Initial measurements<sup>9</sup> of the relaxation time  $T_1$  for temperatures up to 100 K indicated discrepancies in the predictions of relaxation via Raman scattering.

\* Partially supported by U. S. Army Research Office (Durham).

<sup>1</sup> J. H. Van Vleck, *Phys. Rev.* **57**, 426 (1940); in *Spin-Lattice Relaxation in Ionic Solids*, edited by A. A. Manenkov and R. Orbach (Harper and Row Publishers, Inc., New York, 1966), p. 46.

<sup>2</sup> I. M. Lifshitz, *J. Phys. USSR* **7**, 215 (1943); **7**, 249 (1943); **8**, 89 (1944).

<sup>3</sup> D. W. Feldman, J. G. Castle, Jr., and G. R. Wagner, *Phys. Rev.* **145**, 237 (1966).

<sup>4</sup> J. G. Castle, Jr., in *Localized Excitations in Solids*, edited by R. F. Wallis (Plenum Press, Inc., New York, 1968), p. 386.

<sup>5</sup> M. D. Sturge, in *Solid State Physics*, edited by F. Seitz, D. Turnbull, and H. Ehrenreich (Academic Press Inc., New York, 1967), Vol. 20, p. 91.

<sup>6</sup> R. E. Shamu, W. M. Hartmann, and E. L. Yasaitis, *Phys. Rev.* **170**, 822 (1968).

<sup>7</sup> D. W. Feldman, M. Ashkin, and J. H. Parker, *Phys. Rev. Letters* **17**, 1209 (1966).

<sup>8</sup> A. A. Maradudin, in *Localized Excitations in Solids*, edited by R. F. Wallis (Plenum Press, Inc., New York, 1968), p. 1.

<sup>9</sup> J. G. Castle, Jr., D. W. Feldman, and P. G. Klemens, in *Advances in Quantum Electronics* (Columbia University Press, New York, 1961), p. 414.

Our preliminary measurements to 150 K were accounted for<sup>10</sup> by an approximation to the sum over the optical phonons reported<sup>11</sup> in the vibronic spectrum of  $\text{Cr}^{3+}$  in  $\text{MgO}$ . We have now extended the experiment to 430 K. An observed linear variation of  $1/T_1$  with  $T$  above 350 K indicates the relaxation is dominated by strongly anharmonic modes. A single function recently predicted<sup>12</sup> to describe the spin relaxation due to a tunneling oscillator conforms to all the high-temperature data.

From the standpoint of experimental techniques it is interesting to note that line broadening and pulse saturation were both measured in the same temperature range, as discussed in Sec. III. The overlap of the two kinds of data improves the accuracy and reliability of the linewidth method of indirectly determining relaxation time.

## II. EXPERIMENTAL

### A. Summary of $\text{MgO}:\text{Cr}^{3+}$ Resonance

Although  $\text{Cr}^{3+}$  is a  $S' = \frac{3}{2}$  system, all three  $\Delta m = 1$  transitions for the cubic site in  $\text{MgO}$  occur within one line, and the system often behaves<sup>13</sup> as if it were effectively  $S' = \frac{1}{2}$ . The cubic site resonance occurs<sup>14</sup> at about  $g = 1.98$ ; there is some temperature dependence of  $g$  reflecting the thermal expansion of the lattice.<sup>15</sup> There are other Cr resonance lines due to noncubic sites, as well as other Cr isotopes. Other impurities always present in  $\text{MgO}$  lead to many additional resonances.<sup>16</sup> The impurity most likely to interfere with relaxation time measurements is  $\text{Fe}^{2+}$ , because it has a very fast relaxation time.<sup>17</sup> When present in high concentration, or in a strained crystal, the  $\text{Fe}^{2+}$  line can extend above  $g = 2$ .

The spin relaxation of the  $\text{Cr}^{3+}$  ion has been a subject of some interest.<sup>18</sup> Both the direct process<sup>19</sup> and the Raman process<sup>9</sup> below 100 K have been measured for the  $\text{MgO}:\text{Cr}^{3+}$  system. Ultrasonic measurements of the spin-lattice interaction of  $\text{Cr}^{3+}$  in  $\text{MgO}$  have been reported by Shiren.<sup>20</sup>

### B. Samples

Measurements were made on two samples. Sample I, from a small melt of purified AEC grade powder, had previously<sup>9,19</sup> been selected from many samples on the basis of low-temperature relaxation measurements, and exhibited low concentration of all spins. The separation between the peaks of the first derivative of the cubic site  $\text{Cr}^{3+}$  resonance absorption at 40 K is  $0.20 \pm 0.01$  G, but the line shape is rather unusual. Due to the narrow lines, the  $\text{Cr}^{3+}$  resonance is resolved from other resonance lines in the sample at 9.2 GHz. Hole burning was observed at 4.2 K, indicating the line is inhomogeneously broadened. A single measurement at 35 GHz on a chip from the same sample showed an  $H^2$  dependence of  $T_1$ , verifying that the relaxation up to 20 K was due to a direct process.<sup>21</sup>

Sample II, from a large melt, contained 15-ppm  $\text{Cr}^{3+}$  and normal concentrations of other iron-group impurities. The linewidth at 40 K was about 2 G. It was necessary to raise the spectrometer frequency to 9.5 GHz to separate the cubic  $\text{Cr}^{3+}$  line from the nearest  $\text{Mn}^{2+}$  resonance. This sample did not exhibit intrinsic spin relaxation below 90 K, but above 90 K all  $T_1$  measurements coincided with those of Sample I.

### C. Recovery from Pulsed Saturation

The technique of monitoring recovery from pulsed saturation<sup>22,23</sup> was carefully used to measure spin relaxation from 40 to 180 K. An EPR spectrometer which incorporates a traveling wave tube (TWT) receiver<sup>24</sup> was used to make relaxation measurements with a wide signal bandwidth. The spectrometer has the following characteristics: linearity  $\pm 0.5$  dB over a 40-dB range; noise figure 7 dB; rf bandwidth 3 GHz; video bandwidth 15 MHz; internal recovery times, excluding the sample cavity, less than  $0.1 \mu\text{sec}$ . The cavity is a rectangular reflection cavity resonating in the  $TE_{102}$  mode. The decay of the stored energy in the cavity with a loaded  $Q$  of 3000 limited the shortest observable sample relaxation to a  $T_1$  of  $0.5 \mu\text{sec}$ . The system consistently measured the time constant of single exponent recoveries to an accuracy of  $\pm 10\%$ .

The experiment was performed primarily at 9.2 GHz, although measurements on sample II were taken at 9.5 GHz. The resonance was saturated with 10 mW of pulsed power and monitored at powers varying from 10 nW to  $10 \mu\text{W}$ .

Photographs were taken of the oscilloscope trace for each recovery. The difference between the signal  $S(t)$  at time  $t$  and the signal  $S(\infty)$ , long after the pulse, was plotted vs  $t$  on semilog paper, and  $T_1$  was calculated from the slope of the resulting line as illustrated in Fig.

<sup>10</sup> R. L. Hartman, A. C. Daniel, J. S. Bennett, and J. G. Castle, Jr., *Bull. Am. Phys. Soc.* **11**, 313 (1966).

<sup>11</sup> G. F. Imbusch, W. M. Yen, A. L. Schawlow, D. E. McCumber, and M. D. Sturge, *Phys. Rev.* **133**, A1029 (1964); Stanford Technical Report No. 1190, 1964 (unpublished).

<sup>12</sup> J. Murphy, *Phys. Rev.* **145**, 214 (1966).

<sup>13</sup> J. E. Wertz and P. Auzins, *Phys. Rev.* **106**, 484 (1957).

<sup>14</sup> William Low, in *Solid State Physics*, edited by F. Seitz and D. Turnbull (Academic Press Inc., New York, 1960), Suppl. 2.

<sup>15</sup> Walter M. Walsh, Jr., Jean Jeener, and N. Bloembergen, *Phys. Rev.* **139**, A1338 (1965).

<sup>16</sup> An excellent review is given by B. Henderson and J. E. Wertz, *Advan. Phys.* **17**, 749 (1968).

<sup>17</sup> E. L. Wilkinson, R. L. Hartman, and J. G. Castle, Jr., *Phys. Rev.* **171**, 299 (1968).

<sup>18</sup> See list contained in Ref. 19.

<sup>19</sup> J. G. Castle, Jr., and D. W. Feldman, *Phys. Rev.* **121**, 1349 (1961).

<sup>20</sup> N. S. Shiren, in *Magnetic and Electric Resonance and Relaxation*, edited by J. Smidt (North-Holland Publishing Co., Amsterdam, 1963), p. 114 ff.

<sup>21</sup> B. R. McAvoy and J. G. Castle, Jr. (unpublished).

<sup>22</sup> R. H. Dicke and R. H. Romer, *Rev. Sci. Instr.* **26**, 915 (1955).

<sup>23</sup> K. D. Bowers and W. B. Mims, *Phys. Rev.* **115**, 285 (1959).

<sup>24</sup> R. L. Hartman, J. S. Bennett, and R. A. Jensen, *Bull. Am. Phys. Soc.* **13**, 244 (1968).

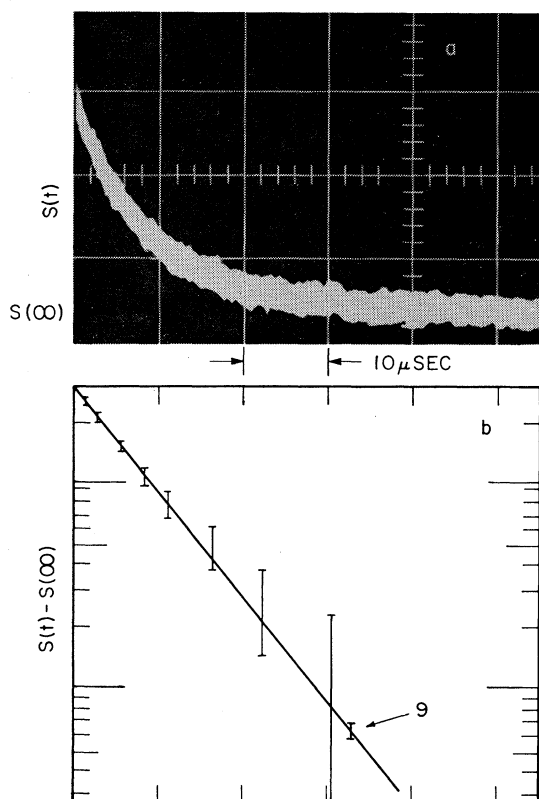


FIG. 1. (a) An oscillograph of the peak of the cubic  $\text{Cr}^{3+}$  line after the termination of the saturating pulse, typical of a fast recovery without signal processing. The time scale is  $10 \mu\text{sec}/\text{cm}$ . Sample conditions:  $T = 99.3 \text{ K}$ ,  $H = 3233 \text{ G}$ ,  $H_0$  along  $[100]$ . The signal  $S(t)$  displayed on the oscilloscope was monitored at four  $\mu\text{W}$  input to the sample cavity. The scale for  $S(t)$  is  $5 \text{ mV}/\text{cm}$ . (b) The deviation from the equilibrium signal  $S(\infty)$ , on a log scale shows that the recovery is given by a single exponential with the relaxation time constant of  $8.6 \mu\text{sec}$ . The single point labeled "9" shows the improved accuracy of the measurements with signal processing.

1. This was judged to give  $T_1$  within  $\pm 10\%$ . A sampling of points was later remeasured and analyzed using more sophisticated signal averaging and computing techniques,<sup>17,24</sup> and each point was found to agree with the original measurements. The improved signal to noise allowed the recovery to be followed to within  $3\%$  of the initial perturbation.

#### D. Measurement of Line Profile

Relaxation measurements were extended to higher temperatures and shorter times by measuring the lifetime broadening of the lines. Because it was necessary to measure the profile of the narrow line to about 1 part in  $10^6$  of applied field, some discussion of experimental precautions is in order here. The lock-in amplifier was especially balanced and aligned to minimize noise. The X-Y recorder gain was set high enough so that the pen chattered slightly, removing mechanical friction as a source of error. The modulation amplitude was care-

fully tested not to affect the measurement. The difficulties arising from the hysteresis and nonlinear sweep of a current controlled magnet and power supply were overcome by measuring the line profiles using a proton resonance gaussmeter which automatically followed the magnetic field. The proton resonance frequency was measured by a counter, and the last three digits converted to an analog signal which drove the  $x$  axis of the recorder. Tracking of  $x$ -axis displacement with magnetic field and other aspects of the measurement technique contributed no more than  $1\%$  to the linewidth measurements.

Conversion of line profiles to absolute values of relaxation times was accomplished by measuring both the line broadening and recovery from pulsed saturation over a common temperature range from  $130$  to  $180 \text{ K}$ . The overlap was permitted by the combination of the very narrow EPR line and the ability of the spectrometer to measure short relaxation times. The linewidth analysis is described in Sec. III.

#### E. Temperature

Temperatures from  $40$  to  $430 \text{ K}$  were measured with a copper constantan thermocouple<sup>25,26</sup> using an ice-water reference junction. The thermocouple emf was measured by using a voltage-to-frequency converter and a frequency counter. This afforded  $10^8\text{-}\Omega$  impedance and  $0.1\text{-}\mu\text{V}$  resolution. Metal bars were bonded to the sides of the cavity to increase thermal conductivity from the heating resistors and help ensure an isothermal environment for the crystal. The thermocouple was separated from the sample by the thin copper cavity wall. At each temperature we waited at least  $10 \text{ min}$  after the thermocouple indicated a constant temperature, in order for the sample to reach the same equilibrium temperature. Calibration to liquid He,  $\text{N}_2$ , and ice water indicated that the uncertainty of the temperature measurement was about  $1\%$ . As  $T_1$  varied no faster than  $T^8$ , a temperature measurement to  $\pm 1\%$  added no more uncertainty than the  $\pm 10\%$  in  $T_1$  measurement.

### III. RESULTS

Figure 1 shows a typical recovery of the peak of resonance absorption following pulsed saturation for the cubic site  $\text{Cr}^{3+}$  in  $\text{MgO}$ . For saturation of the center of the line, single exponential recoveries were observed on photographs at all temperatures. Later use of signal averaging techniques confirmed that at least the first  $97\%$  of the recovery occurs with a single time constant.

Once in each decade of time the measured  $T_1$  was tested and found to be independent of monitor power and pulse width as used. Below  $100 \text{ K}$ ,  $T_1$  values agree

<sup>25</sup> R. L. Powell, M. D. Bunch, and R. J. Corruccini, *Cryogenics* **1**, 139 (1961).

<sup>26</sup> Reference Tables for Thermocouples, Natl. Bur. Std. (U. S.) Circ. No. 561, 35 (1955).

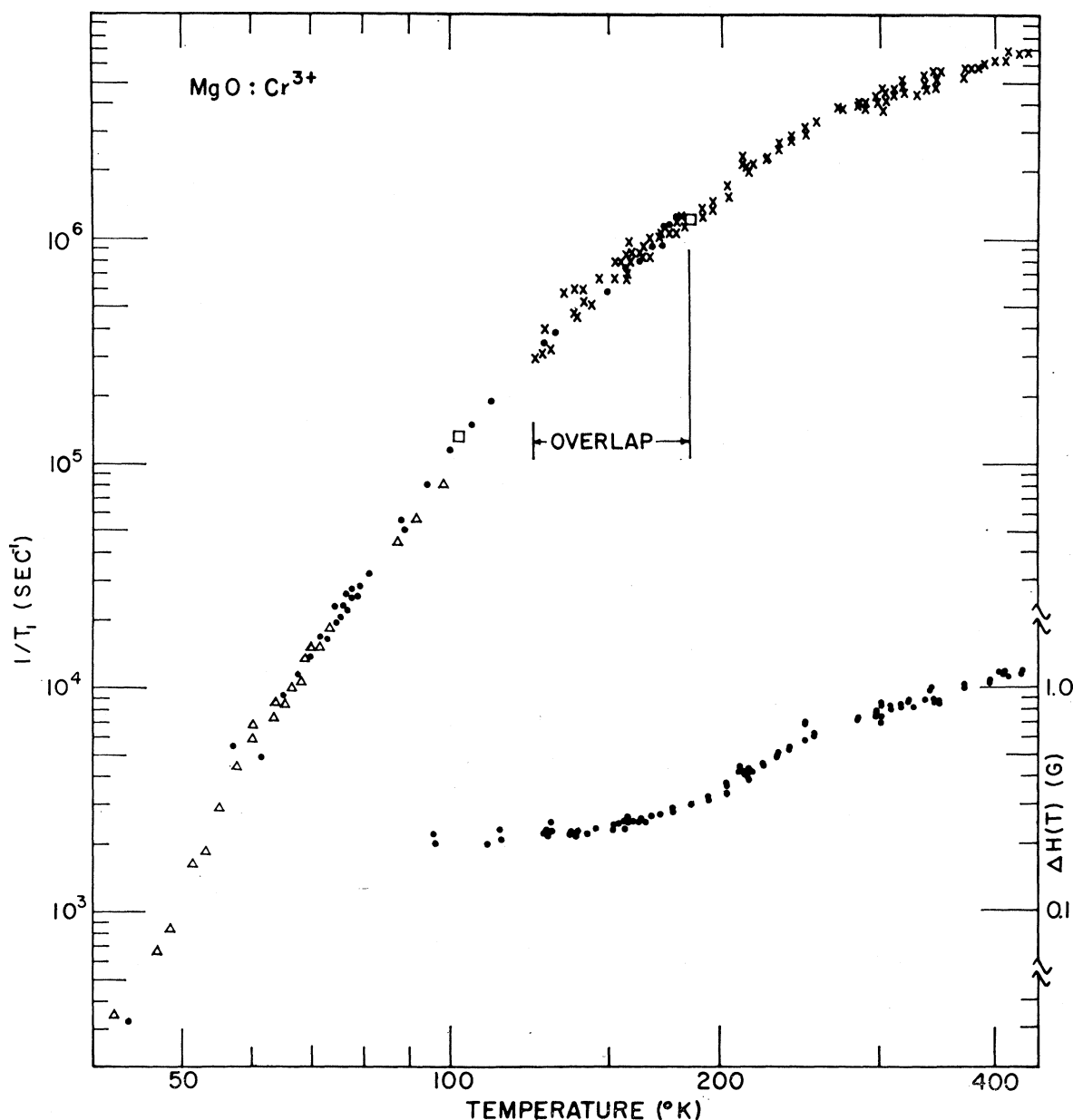


FIG. 2. The reciprocal of the observed relaxation time for the cubic  $\text{Cr}^{3+}$  EPR line in  $\text{MgO}$ , versus lattice temperature  $T$ . Data taken after pulsed saturation are shown by  $\bullet$  for sample I, the low-concentration sample, and by  $\square$  for sample II. The separation between the peaks of the first derivative  $\Delta H(T)$  of the cubic  $\text{Cr}^{3+}$  EPR line is plotted as a function of temperature at the lower right. The relaxation times deduced from this data in the manner described in the text are shown in the main figure with the symbol  $\times$ . For comparison, the previously published data (by permission of Ref. 9), taken by field sweep-inversion recovery, are shown by  $\Delta$ .

to within the  $\pm 10\%$  uncertainty with published data<sup>9,19</sup> taken by field sweep-inversion recovery<sup>27</sup> on the sample. The cubic site  $\text{Cr}^{3+}$  relaxation time  $T_1$  was observed to be independent of angle at 77 K. Angular independence was further verified by spot checks from  $0^\circ$  to  $15^\circ$  in the range 77 to 150 K.

<sup>27</sup> J. G. Castle, Jr., P. F. Chester, and P. E. Wagner, Phys. Rev. 119, 953 (1960).

The relaxation times plotted in the range 40–180 K in Fig. 2 were measured by pulsed saturation. The standard deviation of 8% agrees well with the estimated accuracy of measuring a single recovery.

Relaxation times above 130 K were calculated from an analysis of the temperature dependence of the separation of the two peaks of the first derivative of the absorption line,  $\Delta H(T)$ . The observed values of  $\Delta H(T)$

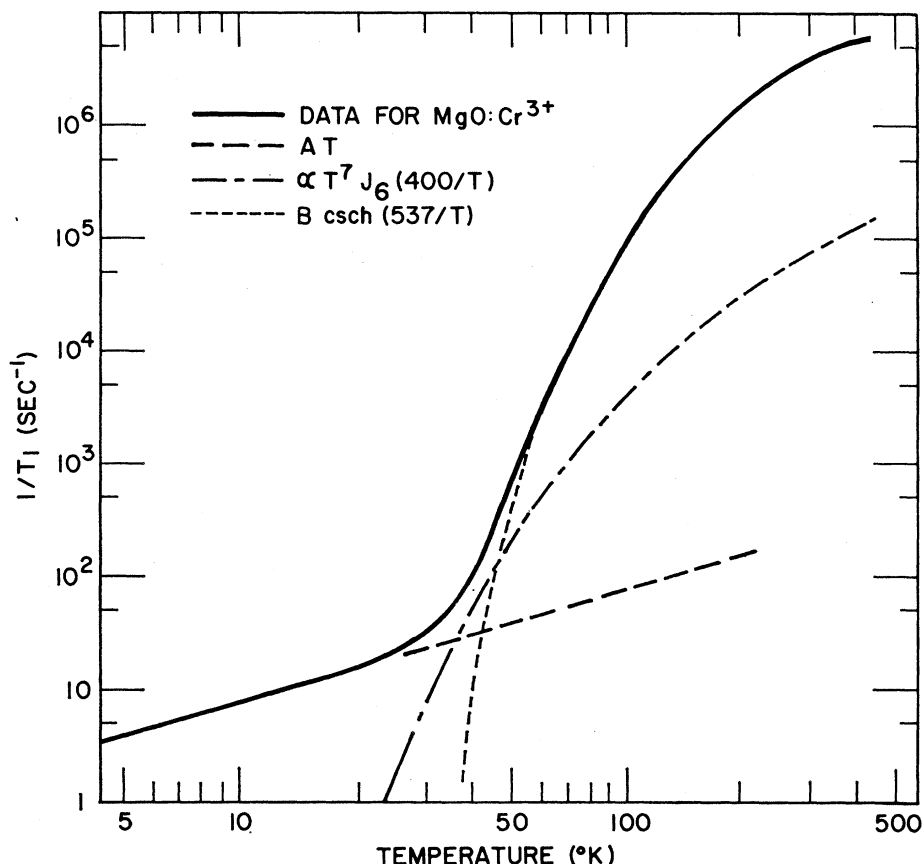


FIG. 3. Contributions to the functional fit of Eq. (2). We plot one specific choice of  $F(n)$ , namely, a contribution due to the acoustical phonons of the lattice. It is obvious from this figure how poorly  $F(n)$  is defined by the data. Also of significance is the dominance of the csch function in the upper temperature range.

are plotted in the lower right corner of Fig. 2. Every analysis relating linewidth to relaxation times involves assumptions which may not be valid.<sup>28-30</sup> The  $\text{Cr}^{3+}$  line shape below 180 K is neither Gaussian nor Lorentzian. Without a tested model for the absorption line, we choose the approximation that a single lifetime describes the line broadening for every cubic  $\text{Cr}^{3+}$  transition at a given  $T$ . The value of this lifetime,  $\tau$ , is taken to be inversely proportional to  $\{[\Delta H(T)]^2 - [\Delta H(0)]^2\}^{1/2}$ , the only one of the usual<sup>31</sup> forms which produces the same variation with temperature from 130 to 180 K for  $\tau$  as is observed for  $T_1$ . The relationship between  $\tau$  and  $T_1$  is taken to be independent of  $T$ . The value of  $T_1$  from line broadening calculated by

$$1/T_1 = \epsilon \{[\Delta H(T)]^2 - [\Delta H(0)]^2\}^{1/2} \quad (1)$$

is shown by  $\times$  in Figs. 2 and 4. The proportionality constant  $\epsilon$  is found to be  $5.8 \times 10^6 \text{ sec}^{-1} \text{ G}^{-1}$  by the overlap with the recovery data below 180 K.

The rapid temperature dependence of  $T_1$  at high  $T$  usually indicates a phonon scattering (Raman) pro-

cess. A resonant scattering (Orbach) process is ruled out for  $\text{MgO}:\text{Cr}^{3+}$  by the absence of electronic states with energy levels within the phonon spectrum.<sup>11</sup> Two features of the data eliminate conventional phonon scattering approaches for calculating the functional dependence of  $T_1$  on  $T$ . Any summation of functions of the form  $T^n J_{n-1}(\theta/T)$  with  $n \leq 7$  does not vary fast enough with  $T$  at 60 K. Furthermore, both the  $T^n J_{n-1}$  for any  $n$ , and any sum of Einstein functions of the form  $e^x/(e^x - 1)^2$ , where  $x = \theta/T$ , are too steep above 300 K, namely, because they vary at least as rapidly as  $T^2$ .

An excellent fit to the data is afforded by

$$1/T_1 = AT + F(n) + B \text{csch}(\Delta/T), \quad (2)$$

with  $A = 0.93 \text{ sec}^{-1}$ ,  $B = (1.20 \pm 0.02) \times 10^7 \text{ sec}^{-1}$ ,  $\Delta = 537 \pm 5 \text{ K}$ . The stated uncertainties in  $B$  and in  $\Delta$  are the standard errors<sup>32</sup> calculated by a least-squares fit to the values of  $T_1$  above 75 K. The value of  $A$  was previously reported.<sup>19</sup> The csch form of relaxation function was originally suggested<sup>12</sup> for a tunneling oscillator, in connection with trapped hydrogen atoms.

Figure 3 shows that the term  $F(n)$  contributes measurably to the relaxation only in the narrow temperature

<sup>28</sup> H. J. Stapleton and K. L. Brower, Phys. Rev. **178**, 481 (1969).

<sup>29</sup> J. W. Culvahouse and P. M. Richards, Phys. Rev. **178**, 485 (1969).

<sup>30</sup> R. L. Hartman and J. S. Bennett, Bull. Am. Phys. Soc. **13**, 1700 (1968).

<sup>31</sup> D. W. Posener, Australian J. Phys. **12**, 184 (1959).

<sup>32</sup> We use the definitions which relate standard deviation to the width of the distribution and standard error to the precision of the mean.

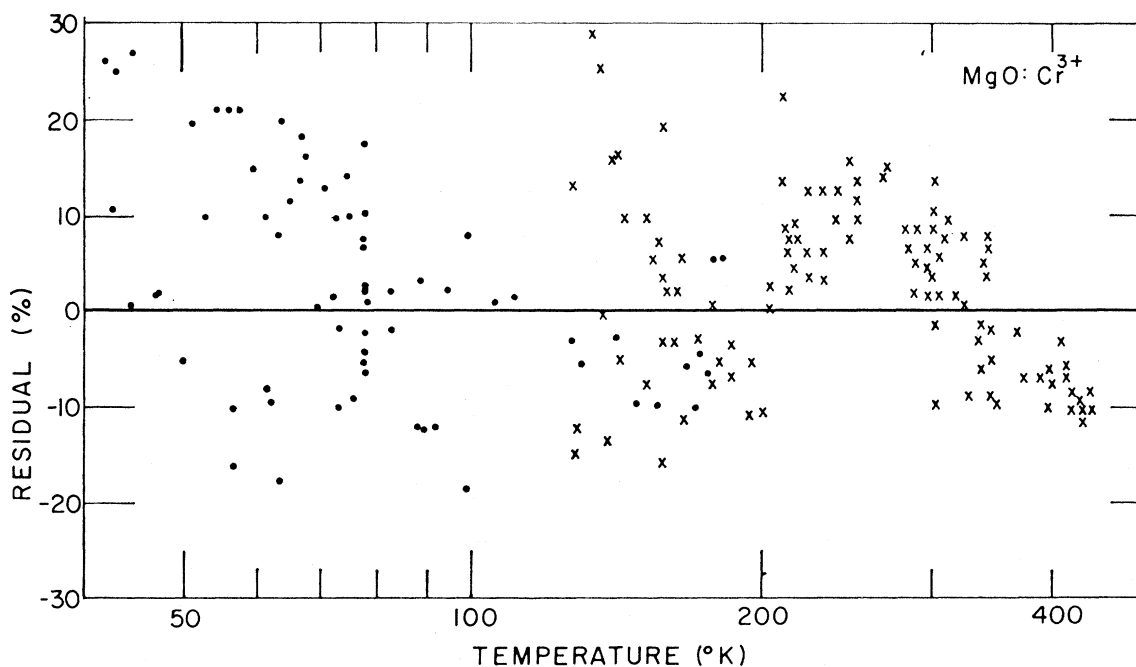


FIG. 4. Demonstration of the accuracy of the fit of Eq. (2) to the data. Plotted here is the residual, Eq. (4), as a function of temperature. Note that there is no systematic deviation outside the limits of the statistical deviation. Pulsed saturation points are shown by ●, and line broadening points by X.

range 30–60 K. This range is sufficiently small that a variety of functions will serve; for example, one may use  $F(n) = 1 \times 10^8 T^{6.2}$ . However, the parameters should be consistent with the known phonon spectrum and the functions should be associated with physical models. Any of the following forms for  $F(n)$  give an adequate fit to the data:

$$T^7 J_6(400/T), \text{ derived for acoustic phonons of MgO; } \quad (3a)$$

$$T^5 J_4(700/T), \text{ derived (Ref. 33) for a Debye approximation to the complete phonon spectrum of MgO; } \quad (3b)$$

$$\sum \rho_i^2 \exp x_i (\exp x_i - 1)^{-2} \text{ for } \rho_i \text{ versus } x_i \text{ from neutron scattering (Ref. 34) of MgO. } \quad (3c)$$

$$\text{The same for } \rho_i \text{ versus } x_i \text{ determined optically (Ref. 11), } \quad (3d)$$

where  $\rho_i$  is the phonon density of states at frequency  $\omega_i$ , and  $x_i = \hbar \omega_i / kT$ .

Since the scale of Fig. 2 ranges over many decades, it is difficult to show the accuracy of the fit of Eq. (2) to the data. For the convenience of the reader, a plot of the residual

$$R = [1/T_1(\text{expt}) - 1/T_1(\text{theoret})]/1/T_1(\text{expt}) \quad (4)$$

is given in Fig. 4. The standard deviation of Eq. (2) is

<sup>33</sup> R. Orbach and M. Blume, Phys. Rev. Letters **8**, 478 (1962).

<sup>34</sup> G. Peckham, Proc. Phys. Soc. (London) **90**, 657 (1967).

8%, and Fig. 4 shows that any apparent systematic deviation of Eq. (2) from the data is no larger than the  $\pm 8\%$  limits. The validity of Eq. (1) for converting linewidth to  $T_1$  is demonstrated by Fig. 4.

Figure 4 can also be used to illustrate the discrepancy for any of the harmonic Raman processes. In this class of processes the closest fit to the data is obtained by the expression for relaxation via a narrow band of Einstein oscillators,  $G \exp(510/T) [\exp(510/T) - 1]^{-2}$ . The function deviates from the data by less than 10% up to 200 K but by more than 30% (off scale on Fig. 4) above 300 K because it varies as  $T^2$  and the data vary as  $T$  in this range.

#### IV. DISCUSSION

Noteworthy features of these relaxation measurements include: (1) each recovery from pulsed saturation being accurately a single exponential, (2) independence of the time constant with respect to several conditions, (3) a direct comparison of lifetime from line broadening with relaxation time constant from pulsed saturation, (4) a temperature dependence significantly weaker than  $T^2$  above 350 K, and (5) relatively weak contributions from normal Raman processes around 40 K. These features are discussed to show the foundations of the conclusions.

##### A. Value of $T_1$

It should be recalled from Sec. III that for a few recoveries integrated by repetitive time sampling, the

logarithm of the deviation from the equilibrium absorption signal was linear with time over a full factor of 30 in the deviation. The noise level in the recoveries was such that if the recovery were to be described by two exponential terms having equal coefficients, then the two decay constants would differ by less than a factor of 2.

In an ion with  $N$  levels in its ground state, recovery from pulsed saturation can be described by a single exponent when either a spin temperature is maintained during recovery by strong spin-spin coupling, or the  $N-1$  characteristic decay constants are approximately equal, or the particular perturbation produced by the saturating pulse does not allow the observation of the  $N-1$  decay constants. A "hole" burned into the narrow cubic  $\text{Cr}^{3+}$  line at low temperatures heals almost independently of the rest of the line, showing that spin-spin coupling does not maintain a spin temperature during these recoveries. Different experiments would be required to distinguish between the other alternatives for the single exponent character of the recoveries.

The observed recovery is judged to be characteristic of the intrinsic spin-lattice relaxation for  $\text{Cr}^{3+}$  in MgO because of the agreement between these two samples above 90 K and the agreement of pulsed saturation data with the previous field sweep-inversion recovery measurements on sample I. Above 77 K the relaxation is constant with respect to angle and field near 3 kG.

To our knowledge, the data taken at temperatures around 150 K by line broadening and by recovery from pulsed saturation represent a new feature. Comparison of the two types of data permit empirical determination of the absolute scale of the effective relaxation time due to finite lifetimes within the  $\text{Cr}^{3+}$  quartet. Therefore, in the remainder of the discussion the values of  $T_1$  plotted in Fig. 2 will be treated as the number which characterizes relaxation of  $\text{Cr}^{3+}$  in MgO at 3 kG at any given  $T$  up to 430 K.

### B. Temperature Dependence

It is clear from Sec. III that no combination of harmonic Raman scattering functions can fit the observed values of  $T_1$  from 350 to 430 K, because the data show a linear temperature dependence. So we conclude that the relaxation of  $\text{Cr}^{3+}$  in MgO above room temperature is due to an extraordinary kind of relaxation process. Two possible cases come to mind. One case would involve Raman scattering between two vibrations which become increasingly anharmonic as  $T$  increases. Such anharmonic vibrations must be associated with a localized mode, because the lattice is still harmonic at 300 K. However, it seems unlikely the anharmonic corrections would change the temperature dependence of  $1/T_1$  from  $T^2$  to precisely  $T$  above 300 K.

The other case involves scattering between harmonic lattice phonons (near the energy of  $370\text{ cm}^{-1}$ ) and a localized vibration with temperature-independent am-

plitude. Such a mode presumably would involve only a few atoms vibrating with large amplitudes. Murphy<sup>12</sup> has discussed two forms of the potential energy which give effectively temperature-independent amplitudes, a square-well potential and the potential function of two widely separated weakly coupled harmonic oscillators. The functions derived for these two cases have very similar temperature dependences if the energy levels are widely spaced as they apparently are for  $\text{Cr}^{3+}$  in MgO. We choose to discuss the localized vibration only in terms of the convenient csch function associated with the coupled harmonic oscillators, remembering that the square-well relaxation function would do almost as well in fitting the  $\text{Cr}^{3+}$  data. It should be noted that relaxation analysis using a multivalleyed harmonic potential with the first eigenvalue of the unperturbed vibrational energy equal to  $\Delta$  also gives  $1/T_1 \propto \text{csch}(\Delta/T)$  provided  $\Delta$  is much larger than the splitting due to the vibration between equivalent wells, i.e., provided  $\Delta \gg \hbar$  times any of the tunneling frequencies.

Adjusting only the two parameters, we noted in Sec. III that the equation  $1/T_1 = B \text{csch}(\Delta/T)$  fits all the data beautifully (i.e., within the experimental uncertainty of  $\pm 8\%$ ) for  $T > 75\text{ K}$ . The standard deviation of this simple equation from the data points gets noticeably worse as the value of  $\Delta$  is taken outside the range of  $537 \pm 5\text{ K}$ .

The consequence of fitting the csch function to the  $T_1$  measured at all  $T$  above 75 K is to place a low value on the maximum contribution from normal Raman scattering. Therefore, the form of the normal Raman term [from the choice of Eq. (3)] is uncertain. The observed values as stated in Sec. III do not distinguish between a  $T^7$  and a  $T^5$  term<sup>33</sup> since that term contributes as much as half of the total Raman scattering only from 30 to 40 K.

### C. Likely Mechanisms

The possible sources of the large-amplitude localized motion which appears to dominate the spin-lattice coupling between  $\text{Cr}^{3+}$  ions and their MgO host crystal merit some speculative discussion. Static relaxation of the six nearest-neighbor oxygens in toward the extra charge of the  $\text{Cr}^{3+}$  is expected; the associated static relaxation of the succeeding layers of neighbors would tend toward isolating the  $\text{CrO}_6$  complex from its host. Thus some motions within the  $\text{CrO}_6$  complex may be able to reach large amplitudes in spite of the existence of MgO modes of the same frequency.

It is interesting to note that the value of the frequency for the csch function lies near a sharp edge between high- and low-density regions in the effective phonon spectrum as seen in the vibronic sidebands of the  $R$  line of  $\text{Cr}^{3+}$  in MgO.

A likely source of the localized motion at  $1.1 \times 10^{13}\text{ Hz}$  (537 K) is molecularlike hindered rotational motions of the  $\text{CrO}_6$  complex around a  $[111]$  axis, as suggested

to us by Stettler. Excellent discussions of the strength and frequencies of Jahn-Teller distortions have recently been written,<sup>5,35</sup> indicating the  $\text{Cr}^{3+}$  ground state is not effected directly and therefore does not give rise to this localized motion.

### V. CONCLUSIONS

Within the  $S' = \frac{3}{2}$  ground state of  $\text{Cr}^{3+}$  ions in cubic sites in  $\text{MgO}$  at any given temperature over the range 40–180 K, the recovery from pulsed saturation is accurately described by a single relaxation time constant. No explanation of this is offered by these data.

The  $\text{Cr}^{3+}$  relaxation time near 3 kG is accurately given by the function  $\text{csch}(537/T)$  at all values of  $T$  from 75 to 430 K. Every other relaxation function based on either of the two measured phonon spectra or on a single Einstein mode exhibits systematic deviations

from the observed values much larger than the random experimental uncertainty based on measured signal to noise and confirmed by the statistics of repeated recoveries at each  $T$ . The  $\text{csch}$  function suggests relaxation via localized modes having temperature-independent amplitudes such as might be possible in motions of the  $\text{CrO}_6$  complex.

With the high-temperature relaxation fitted, the expected harmonic Raman relaxation functions account for more than 50% of the observed relaxation only in the range between 30 and 40 K, temperatures corresponding to less than 10% of the energy of the transverse acoustic peak. Apparently motions localized around each  $\text{Cr}^{3+}$  ion dominate the ground-state relaxation.

### ACKNOWLEDGMENTS

We especially appreciate discussions on the theory with F. S. Ham, J. Murphy, and J. D. Stettler. We acknowledge valuable contributions from A. C. Daniel, D. W. Feldman, R. A. Shatas, and E. L. Wilkinson.

<sup>35</sup> F. S. Ham, in *Electron Paramagnetic Resonance*, edited by S. Geschwind (Plenum Press, Inc., New York, to be published). Ham's chapter may also be available as Report No. 68C246 from General Electric Research and Development Center, Schenectady, N. Y. (unpublished).

## $\text{Rb}^{87}$ and $\text{As}^{75}$ Quadrupolar Coupling in Ferroelectric $\text{RbH}_2\text{PO}_4$ and $\text{CsH}_2\text{AsO}_4$ †

R. BLINC,\* D. E. O'REILLY, AND E. M. PETERSON

Argonne National Laboratory, Argonne, Illinois 60439

(Received 15 October 1969)

The quadrupole-induced shifts of the  $\text{Rb}^{87}$  and  $\text{As}^{75}$   $\frac{1}{2} \leftrightarrow -\frac{1}{2}$  nuclear-magnetic-resonance transitions have been used to study the temperature variation of the electric field gradients at the ionic sites on approaching the ferroelectric Curie points. The shifts can only be explained in terms of collective atomic fluctuations in the paraelectric phase. A soft-lattice-mode model does not quantitatively describe the temperature dependence of the frequency shifts. A model which explicitly takes into account the protonic disorder accounts quantitatively for the arsenic data. No quantitative treatment that is in good agreement with the rubidium data has been found.

### INTRODUCTION

IT is well known that the ferroelectric transitions in  $\text{KH}_2\text{PO}_4$ -type crystals are accompanied by displacements of the K and P ions in the  $+$  and  $-z$  ( $c$ ) directions, respectively, which accounts for the larger part of the spontaneous polarization. But whereas the proton motion and proton ordering have been investigated in great detail, relatively little is known on a microscopic scale on the motion of the heavy ions in the vicinity of the Curie point. It was often taken for granted that the proton system and the lattice motion are effectively decoupled in the paraelectric state, and that the polar lattice displacements occur only after the

proton ordering takes place. It was only recently that this "rigid" lattice model has been questioned and the importance of the coupling between proton motion and the polar lattice distortions for  $T > T_C$  was pointed out.

This investigation was made in the hope of throwing some additional light on the nature of the proton-lattice coupling in  $\text{KH}_2\text{PO}_4$ -type crystals by studying the temperature variation of the local electric field gradient (EFG) tensors at the Rb and As sites in  $\text{RbH}_2\text{PO}_4$  and  $\text{CsH}_2\text{AsO}_4$ . Together with the available information on the EFG tensor at the  $\text{Cs}^{133}$  site, these data should provide a sensitive test of the various theoretical models proposed so far.

#### A. $\text{As}^{75}$

The quadrupole-induced shifts of the  $\frac{1}{2} \rightarrow -\frac{1}{2}$  magnetic resonance transition of  $\text{As}^{75}$  ( $I = \frac{3}{2}$ ) in  $\text{CsH}_2$ -

† Based on work performed under the auspices of the U. S. Atomic Energy Commission.

\* On leave of absence, University of Ljubljana, Institute "J. Stefan," Ljubljana.



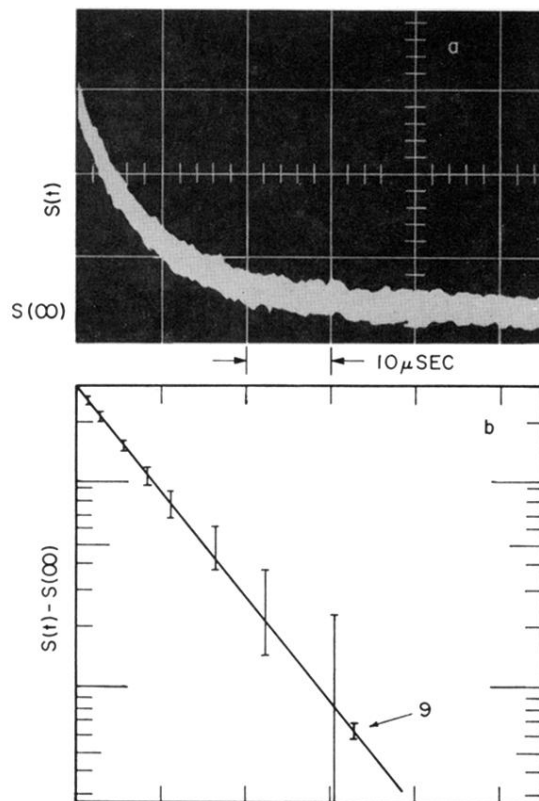


FIG. 1. (a) An oscillograph of the peak of the cubic  $\text{Cr}^{3+}$  line after the termination of the saturating pulse, typical of a fast recovery without signal processing. The time scale is  $10 \mu\text{sec/cm}$ . Sample conditions:  $T = 99.3 \text{ K}$ ,  $H = 3233 \text{ G}$ ,  $H_0$  along  $[100]$ . The signal  $S(t)$  displayed on the oscilloscope was monitored at four  $\mu\text{W}$  input to the sample cavity. The scale for  $S(t)$  is  $5 \text{ mV/cm}$ . (b) The deviation from the equilibrium signal  $S(\infty)$ , on a log scale shows that the recovery is given by a single exponential with the relaxation time constant of  $8.6 \mu\text{sec}$ . The single point labeled "9" shows the improved accuracy of the measurements with signal processing.